Journal of Materials Chemistry A

ROYAL SOCIETY OF CHEMISTRY

PAPER

View Article Online
View Journal

Cite this: DOI: 10.1039/d1ta04517b

Coupling of a new porphyrin photosensitizer and cobaloxime cocatalyst for highly efficient photocatalytic H_2 evolution†

Govardhana Babu Bodedla, [abc] Wai-Yeung Wong [*bc] and Xunjin Zhu [*a]

Photocatalytic hydrogen evolution (PHE) is a promising strategy to produce environmentally friendly clean energy with the use of solar power and water. For this, developing an efficient and noble metal free photocatalytic system (PS) comprising high light-harvesting and photostable photosensitizers is an important and challenging task. Herein, a new porphyrin photosensitizer ZnDC(*p*-NI)PP, containing two naphthalimide (NI) donor chromophores and 4-carboxyphenyl substituents is developed for PHE. Using chloropyridinecobaloxime (CoPyCl) as a cocatalyst in phosphate buffer/THF solution at pH 7.4, the homogeneous PS of ZnDC(*p*-NI)PP exhibits a very high hydrogen evolution rate (η_{H_2}) of 35.70 mmol g^{-1} h^{-1}, turnover number (TON) of 5958 and apparent quantum efficiency (AQE) of 10.01%. This performance recorded under the same conditions is significantly higher than that of the PS of ZnDCPP which lacks the NI moieties (η_{H_2} of 4.64 mmol g^{-1} h^{-1}, TON of 1397 and AQE of 1.30%), the typical PS of ZnTCPP with four 4-carboxyphenyl substituent groups (η_{H_2} of 2.43 mmol g^{-1} h^{-1}, TON of 562 and AQE of 1.00%), and previously reported ZnD(*p*-NI)PP containing only two NI chromophores (η_{H_2} of 3.8 mmol g^{-1} h^{-1}, TON of 590 and AQE of 1.5%). The noticeable performance of ZnDC(*p*-NI)PP in PHE is attributed to the intramolecular energy transfer from the NI donor chromophore to the porphyrin acceptor that would promote the long-lived photoexcitation states. At the same time, the anionic form ($-COO^-$) of 4-carboxyphenyl substituents at pH 7.4 enables a faster electron transfer from the porphyrin group to the cationic Co(III) due to electrostatic force. To the best of our knowledge, the PHE results of ZnDC(*p*-NI)PP represent the best one for porphyrin photosensitizers and cobaloxime PSs reported so far. This work paves a new direction for developing new porphyrin-based materials for efficient PHE through facile molecular structure engineering.

Received 28th May 2021
Accepted 9th August 2021

DOI: 10.1039/d1ta04517b

rsc.li/materials-a

Introduction

Solar light-driven splitting of water into hydrogen as carbon free fuel and environmentally friendly clean energy is a promising strategy for reducing the consumption of natural fossil fuel resources and greenhouse effect.[1–4] To produce photocatalytic hydrogen evolution (PHE), the photocatalytic systems (PSs) should mainly contain three components namely a photosensitizer, sacrificial electron donor and cocatalyst. Based on this multicomponent PS design, Lehn and co-workers reported for the first time decent PHE results using $Ru(bpy)_3^{2+}$ as a photosensitizer, triethanolamine (TEOA) as a sacrificial donor and colloidal Pt as a cocatalyst.[5] After this a huge number of multicomponent homogeneous/heterogeneous PSs have been developed by employing different combinations of photosensitizers such as Ru-, Ir- and Re-based complexes (noble metals),[6–8] inorganic composites,[7,9] porous materials,[10,11] organic small molecules and polymers,[7,12–14] graphitic carbon nitride ($g\text{-}C_3N_4$) polymeric materials,[15,16] porphyrin derivatives[17–20] and their hybrids with $g\text{-}C_3N_4$/graphene oxide[21] and cocatalysts such as colloidal Pt,[7,22] Ni-, Fe- and Co-based complexes[23–27] with the use of sacrificial donors such as triethylamine (TEA), ascorbic acid (AA) and TEOA. Although the PSs comprising either noble metal based photosensitizers or cocatalysts (*e.g.* Pt) produced highly efficient PHE, they cannot be commercialized in the near future due to the high cost of noble metals. To tackle this problem, researchers mainly used noble metal free photosensitizers and cocatalysts for the preparation of PSs. Among the noble metal free photosensitizers, recently, porphyrin derived materials have attracted enormous interest in the PHE owing to their strong

[a]Department of Chemistry and Institute of Advanced Materials, Hong Kong Baptist University, Waterloo Road, Kowloon Tong, Hong Kong, P. R. China. E-mail: xjzhu@hkbu.edu.hk

[b]Department of Applied Biology & Chemical Technology, Research Institute for Smart Energy, The Hong Kong Polytechnic University, Hong Kong, P. R. China. E-mail: wai-yeung.wong@polyu.edu.hk

[c]The Hong Kong Polytechnic University, Shenzhen Research Institute, Shenzhen 518057, P. R. China

† Electronic supplementary information (ESI) available: Materials and methods, synthesis, photocatalytic systems under different conditions, cyclic voltammograms, ^1H and ^{13}C NMR spectra, and MALDI-TOF spectra. See DOI: 10.1039/d1ta04517b

solar light absorbing nature in the maximum UV-vis region, long-lived photoexcited states and possession of suitable HOMO and LUMO energy levels for efficient photoinduced charge separation and their transfer to the cocatalyst.[17,18,28]

On the other hand, cobalt complexes, especially, cobaloximes as cocatalysts have received tremendous interest due to their easy synthesis, reasonable photostability and high PHE efficiencies due to low reduction potential.[25,29] Importantly, understanding of electron transfer between the components of PSs is the main criterion to improve the PHE. For this, preparation of PSs under fully homogeneous conditions is required. Thus development of new PSs comprising porphyrin photosensitizers and the cobaloxime cocatalyst under homogeneous conditions for high performance PHE is not only a prerequisite but also a necessary condition to pave this research field towards our modern society. However, though a very few homogeneous PSs featuring porphyrin photosensitizers and the cobaloxime cocatalyst for PHE have been reported so far, they are not much efficient and stable due to weak light absorbing nature of porphyrins and their photo instability.[30,31] Thus, we aimed to develop highly efficient PSs for PHE by enhancing the light absorbing properties and photostability of porphyrin photosensitizers.

We have recently found that the linear substitution of di-naphthalimide (NI) moieties at the *meso*-position of the porphyrin core greatly improved the light absorption, stability of photoexcited states, photoinduced charge separation and photostability of porphyrin photosensitizers and thus PHE.[32] This could be attributed to the efficient intramolecular energy transfer from the NI energy donor chromophore to the porphyrin energy acceptor. In this study, we used heterogeneous conditions to evaluate the PHE of di-NI conjugated porphyrin, ZnD(*p*-NI)PP with the use of a Pt cocatalyst. Though the PS of ZnD(*p*-NI)PP delivered efficient PHE results, it is not a cost-effective approach and the intrinsic photocatalytic cyclic mechanism was also not much fully addressed due to the usage of Pt and heterogeneous photocatalytic conditions, respectively. In order to prepare cost-effective, efficient and homogeneous PSs, herein we have developed a new porphyrin photosensitizer, ZnDC(*p*-NI)PP bearing two NI donor chromophores and two –COOH groups (Fig. 1) and tested its PHE properties using the chloropyridinecobaloxime (CoPyCl) cocatalyst under homogeneous phosphate buffer/THF conditions. We presume that upon light irradiation ZnDC(*p*-NI)PP porphyrin produces long-lived photoexcited states due to occurrence of energy transfer between the NI donor chromophore and porphyrin acceptor resulting from the overlap between the emission profile of NI and the absorption of the porphyrin moiety. As a result, the ZnDC(*p*-NI)PP efficiently accepts electrons from the sacrificial donor and quickly transfers to CoPyCl where proton reduction takes place. Thus, the PS of ZnDC(*p*-NI)PP porphyrin exhibited a hydrogen evolution rate (η_{H2}) of 35.70 mmol g^{-1} h^{-1}, which is 8-fold higher than that of the control porphyrin ZnDCPP which lacks the NI groups (4.64 mmol g^{-1} h^{-1}) and even 15-fold higher than that of the typical porphyrin, ZnTCPP (2.43 mmol g^{-1} h^{-1}).

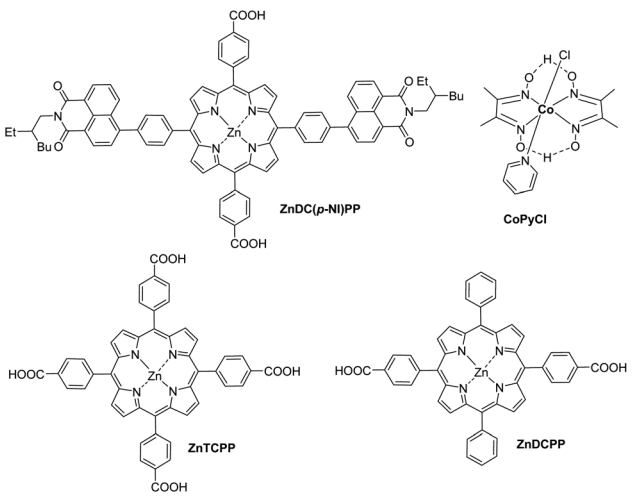

Fig. 1 Structures of the porphyrins used in this study.

Results and discussion

Experimental section

The synthetic protocol used for the preparation of ZnDC(*p*-NI)PP is shown in Scheme 1. The di-bromozinc derivative, DiBrZnD(*p*-NI)PP was synthesized by bromination of D(*p*-NI)PPH_2 with the NBS reagent followed by reaction with $Zn(OAC)_2 \cdot 2H_2O$. Subsequently, reaction of DiBrZnD(*p*-NI)PP with 4-carboxyphenyl boronic acid by the Suzuki–Miyaura coupling reaction yielded the target ZnDC(*p*-NI)PP porphyrin. The control porphyrin ZnDCPP was synthesized in two steps (Scheme S1†). First, the acid catalyzed condensation of phenyl dipyrrolomethane with 4-formylmethylbenzoate produced the DMMPPH2 porphyrin and zinc metalation of this gave ZnDMCPP. In the second step, demethylation of ZnDMCPP under basic conditions resulted in the ZnDCPP porphyrin. Zinc(II)-tetracarboxyphenylporphyrin (ZnTCPP) was synthesized for comparison (Scheme S2†). Both porphyrins were thoroughly characterized by NMR and MALDI-TOF techniques.

Optoelectronic properties

The absorption and emission spectra of the porphyrins are shown in Fig. 2 and the corresponding data are shown in Table

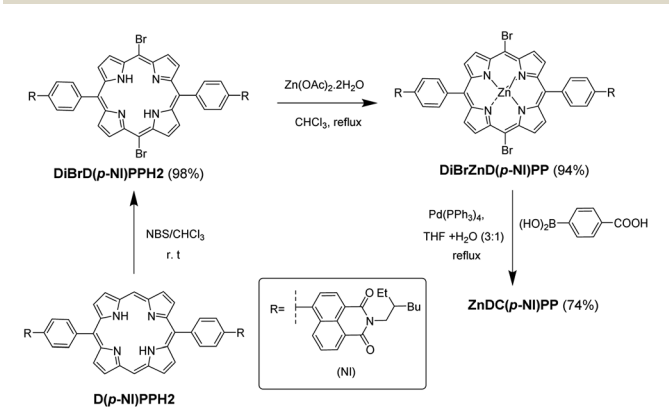

Scheme 1 Synthetic route for the preparation of ZnDC(*p*-NI))PP porphyrin.

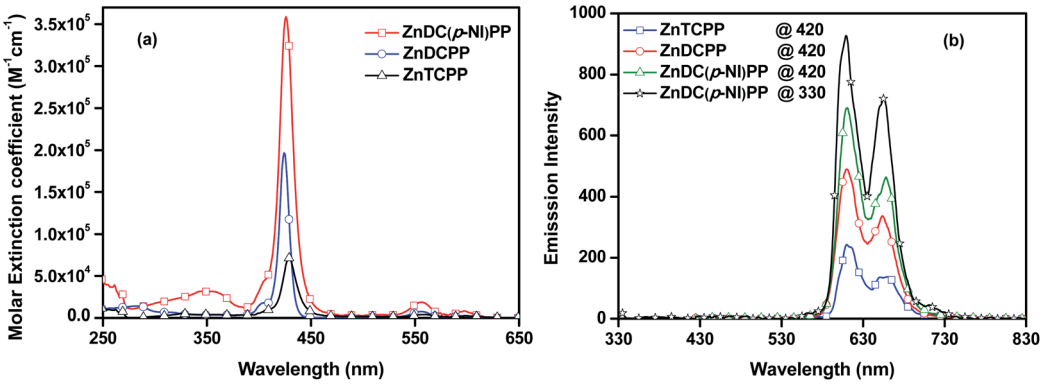

Fig. 2 (a) Absorption and (b) emission spectra of the dyes recorded in phosphate buffer/THF (9 : 1 v/v, 10 μM, pH = 7.4)) solution. All the porphyrins were excited at 420 nm and additionally, ZnDC(*p*-NI)PP was also excited at 330 nm to understand the intramolecular energy transfer between the NI donor and porphyrin acceptor.

1. All the porphyrins mainly show two types of peaks. The broad and intense peaks located at *ca.* 420–440 nm correspond to the Soret band absorption and the less intense peaks positioned at *ca.* 500–650 nm are attributed to the Q-band absorption. For ZnDC(*p*-NI)PP porphyrin, the additional peaks in the higher energy region (*ca.* 350 nm) could be ascertained to the NI absorption peaks. Notably, ZnDC(*p*-NI)PP porphyrin shows apparently higher molar extinction coefficient (ε) values for Soret- and Q-bands than the ZnDCPP which lacks the NI groups and ZnTCPP featuring four carboxylic groups. This could be attributed to the conjugation of NI donor chromophores to the *meso*-positions of the porphyrin acceptor which might affect the electronic transition probability between the $^1S_0$–^1E_u and $^1S_0$–^2E_u transitions of the porphyrin macrocycle.[33] These results clearly indicate that conjugation of NI donor chromophores to the *meso*-position of the porphyrin moiety could enhance the light-harvesting ability in the UV-visible region and consequently could lead to good PHE results. It is noted that ZnTCPP shows a lower ε value for the Soret band than ZnDC(*p*-NI)PP and ZnDCPP.

All the porphyrins show two emission peaks in the region of 600–700 nm under 420 nm excitation which belongs to the Soret band of the porphyrin moiety. The intense emission peaks at *ca.* 610 nm and weak emission peaks at *ca.* 660 nm correspond to the Q(0,0) and Q(0,1), respectively of the porphyrin macrocycle. In our previous reports, we have already demonstrated the occurrence of intramolecular Förster resonance energy transfer (FRET) between NI donor chromophores and the porphyrin acceptor due to the overlapped emission spectrum of NI and the absorption spectrum of the porphyrin ring.[32–34] Accordingly, ZnDC(*p*-NI)PP porphyrin bearing the NI would show FRET between NI moieties and the porphyrin ring. In general, the NI chromophore shows a very strong emission peak at *ca.* 450 nm under 330 nm excitation which corresponds to NI absorption. Impressively, the absence of the NI emission peak in the ZnDC(*p*-NI)PP emission spectrum under 330 nm excitation clearly indicates efficient FRET between the NI donor and the porphyrin acceptor. The calculated FRET efficiency (Φ_{ET}) of ZnDC(*p*-NI)PP is 99%. Since the fluorescence lifetime (t_F) of the porphyrin is directly related to the stability of porphyrin excited states, calculation of t_F could give more insight into the porphyrin photoexcited states (Fig. 3(a)). The order of calculated t_F of the porphyrins is as follows: ZnDC(*p*-NI)PP (3.8 ns) > ZnDCPP (2.4 ns) > ZnTCPP (1.8 ns). Among the three porphyrins, the ZnDC(*p*-NI)PP bearing the NI moieties showed the highest t_F. This obviously indicates that the ZnDC(*p*-NI)PP possesses highly stabilized photoexcited states. The higher t_F of ZnDC(*p*-NI)PP than the ZnDCPP and ZnTCPP could be ascribed to the efficient FRET between NI and porphyrin moieties. Moreover, the control porphyrin, ZnDCPP also shows higher t_F than the commonly used ZnTCPP. This indicates that the porphyrin with two carboxylic groups possesses long lived photoexcited states than the congener porphyrin with four COOH groups. The calculated photoluminescence quantum yield (Φ_F) of the porphyrins is in the order of ZnDC(*p*-NI)PP

Table 1 Optical properties of the dyes recorded in buffer/THF (9 : 1 v/v) solution at pH 7.4

Porphyrin	λ_{abs}[a] ($\varepsilon \times 10^4$, M^{-1} cm^{-1}) (nm)	λ_{em}[a] (nm)	Φ_F[a]	t_F[a] (ns)	E_{Ox}[b] (V)	E_{Red}[c] (V)	$E_{(P^+/P^*)}$[d] (V)	$E_{(P^*/P^-)}$[e] (V)	$E_{0\text{-}0}$[f]
ZnDC(*p*-NI)PP	350 (3.18), 426 (35.88), 556 (1.82), 597 (0.78)	611, 653	0.18	3.8	1.23, 1.53	−1.13	−0.94	1.04	2.17
ZnDCPP	424 (19.66), 556 (0.77), 599 (0.26)	609, 655	0.13	2.4	1.22, 1.54	−1.19	−0.97	1.00	2.19
ZnTCPP	429 (7.15), 560 (0.40), 599 (0.27)	610, 660	0.10	1.8	1.20, 1.48	−0.83, −1.17	−0.95	1.32	2.15

[a] Phosphate buffer/THF (9 : 1 v/v) solution. [b] E_{ox} (*vs.* NHE) = 0.77 + E_{ox} (*vs.* ferrocene). [c] E_{red} (*vs.* NHE) = 0.77 − E_{red} (*vs.* ferrocene). [d] $E_{(P^+/P^*)}$ (*vs.* NHE) = E_{Ox} − $E_{0\text{-}0}$; here "P" refers to the porphyrin photosensitizer. [e] $E_{(P^*/P^-)}$ (*vs.* NHE) = E_{Red} + $E_{0\text{-}0}$. [f] Estimated from the intersection of the normalized absorption and emission spectra.

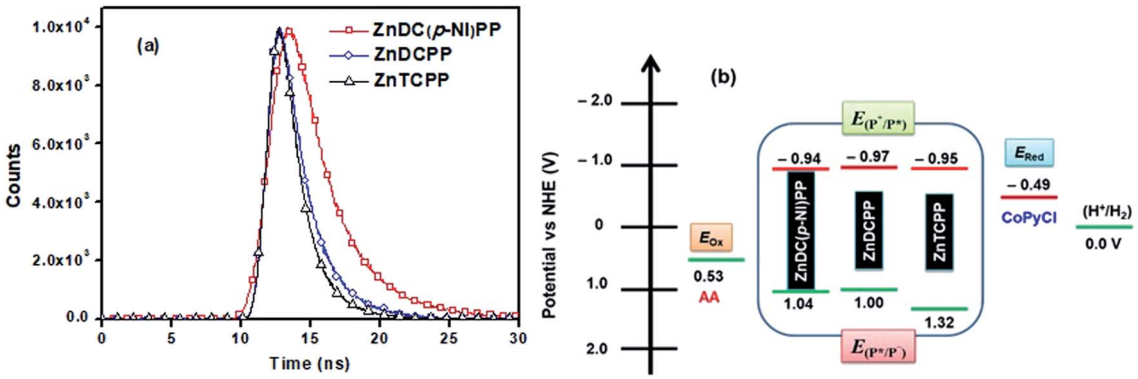

Fig. 3 (a) Lifetime decay spectra of the porphyrins recorded in phosphate buffer/THF (9 : 1 v/v, 10 μM at pH 7.4) solution at room temperature and (b) energy level alignment of the porphyrins, sacrificial donor and water reduction catalyst.

(18%) > ZnDCPP (13%) > ZnTCPP (10%) which is also in line with their t_F trend.

The thermodynamic viability of electron transfer during the PHE cycle depends mainly on the excited state oxidation potentials ($E_{(P^+/P^*)}$) and excited state reduction potentials ($E_{(P^*/P^-)}$) of the porphyrins.[35] Since such relative energies cannot be evaluated directly, first, we calculated the first oxidation potential (E_{Ox}) and first reduction potential (E_{Red}) values which correspond to the HOMO and LUMO of the porphyrins, respectively, by performing the cyclic voltammetric experiments in THF solution (Fig. S1†). The calculated E_{Ox} values of ZnDC(*p*-NI)PP, ZnDCPP and ZnTCPP are 1.23, 1.22, and 1.20 V, respectively. And the values of −1.13, −1.19, and −0.83 V correspond to the E_{Red} of ZnDC(*p*-NI)PP, ZnDCPP and ZnTCPP, respectively. According to the Rehm–Weller equations (see the footnote in Table 1), the ($E_{(P^+/P^*)}$) values of the ZnDC(*p*-NI)PP, ZnDCPP and ZnTCPP were calculated to be −0.94, −0.97, and −0.95 V, respectively and ($E_{(P^*/P^-)}$) values of the porphyrins ZnDC(*p*-NI)PP, ZnDCPP and ZnTCPP were calculated to be 1.04, 1.00, and 1.32 V, respectively. As seen in Fig. 3(b), the ($E_{(P^*/P^-)}$) values of the porphyrins are more positive than the oxidation potential (E_{ox}) of the AA sacrificial electron donor indicating a favourable thermodynamic driving force for electron transfer from AA to photoexcited porphyrins. And the ($E_{(P^+/P^*)}$) values of porphyrins are more negative than the reduction potential (E_{ox}) of the CoPyCl cocatalyst, suggesting an effective transfer of electrons from photoexcited porphyrin to CoPyCl where proton reduction takes place. The relatively high-lying ($E_{(P^*/P^-)}$) value of ZnDC(*p*-NI)PP than the ZnTCPP should be helpful for more efficient electron transfer from AA to photoexcited porphyrins and thus expectably higher PHE performance for ZnDC(*p*-NI)PP than that of ZnTCPP.

PHE studies

In order to evaluate the PHE properties of porphyrins, a series of homogeneous PSs were prepared in buffer/THF solution by employing porphyrins as photosensitizers, AA as the sacrificial electron donor and CoPyCl as the cocatalyst. The optimized PHE properties of PSs are shown in Fig. 4 and the corresponding data are shown in Table 2. Fig. 4(a) shows the hydrogen evolution rate (η_{H2}) of the PSs under the illumination of an OLED light source for 5 h. From Fig. 4(a), it can be noted that the ZnDC(*p*-NI)PP bearing the NI donor chromophores and –COOH groups displayed higher η_{H2} than the ZnDCPP which lacks the NI moieties and well known ZnTCPP. The η_{H2} order of

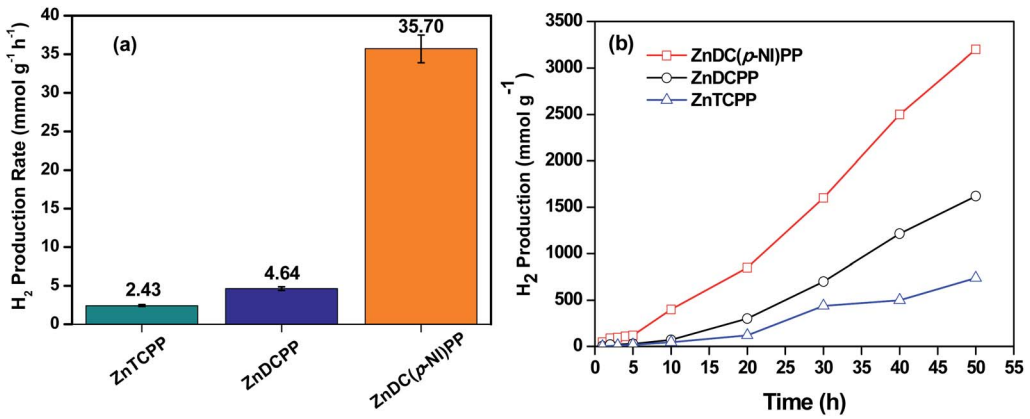

Fig. 4 (a) H_2 production rate of photocatalytic systems under irradiation for 5 h and (b) H_2 production of photocatalytic systems under irradiation (white LED light (148.5 mW cm^{-2})) for 50 h: (porphyrin (10 μM) + CoPyCl (2 mM) + AA (0.4 M) + buffer/THF (9 : 1 v/v) at pH 7.4).

Table 2 Amount of H_2 (η_{H_2}), turnover number (TON), and apparent quantum yield (AQE) of the photocatalytic systems

Porphyrin	η_{H_2} [a] (mmol g^{-1} h^{-1})	TON[b]	AQE%[c]
ZnTCPP	2.43	562	1.00
ZnDCPP	4.64	1397	1.30
ZnDC(*p*-NI)PP	35.70	5958	10.01
ZnD(*p*-NI)PP	3.80	590	1.50

[a] Calculated under irradiation for 5 h. [b] Calculated under irradiation for 50 h. [c] Calculated under irradiation for 1 h.

the PS of the porphyrins is ZnDC(*p*-NI)PP (35.70 mmol g^{-1} h^{-1}) > ZnDCPP (4.64 mmol g^{-1} h^{-1}) > ZnTCPP (2.43 mmol g^{-1} h^{-1}). The calculated apparent quantum yield (AQE) values of ZnDC(*p*-NI)PP, ZnDCPP and ZnTCPP PSs are 10.01%, 1.30% and 1.00%, respectively. The AQE values of PSs also match well with their η_{H2} order. Furthermore, under the optimized conditions, the photostability of the three porphyrin PSs was also evaluated by measuring their PHE up to 50 h of light irradiation. As seen in Fig. 4(b), the PHE of the three porphyrins gradually increased with time indicating the good photostability of all components. The appearance of similar absorption and emission spectra of the PSs before and after light irradiation also attests to their good photostability under light irradiation (Fig. S11 and S12†). The order of turnover number (TON) of the three PSs is as follows: ZnDC(*p*-NI)PP (5958), ZnDCPP (1397) and ZnTCPP (562) which is also in line with their η_{H2} and AQE trends. More importantly, the η_{H2} and TON of ZnDC(*p*-NI)PP PS are superior to those of the PSs comprising porphyrin photosensitizers and cobaloxime catalysts so far in the literature (Table S1†).[30,31,36,37] Particularly, the η_{H2} of the ZnDC(*p*-NI)PP PS is 3.3 times higher than that of the most efficient PS containing the water soluble porphyrin photosensitizer, PorFN (10.9 mmol g^{-1} h^{-1}) and Pt cocatalyst reported recently.[38] Moreover, the η_{H2} of ZnDC(*p*-NI)PP is also much higher than that of our recently reported iridium-conjugated porphyrins[39] and far better than that of the NI-conjugated porphyrins under heterogeneous conditions with the Pt cocatalyst.[32–34] The superior PHE properties of ZnDC(*p*-NI)PP possessing the 5,15-di(NI) substituted porphyrin donor chromophores compared to the ZnDCPP which lacks the NI could be explained by the following factors: (i) good light-harvesting properties in the UV-vis region of the solar spectrum, (ii) efficient FRET from the NI donor to the porphyrin acceptor would stabilize the photoexcited states of the porphyrin ring and thus long-lived photoexcited electron lifetime which further enhances the electron transfer from the photo-excited porphyrin moiety to the CoPyCl through COOH groups, and (iii) an efficient acceptance of electrons from AA and subsequent transfer to CoPyCl (*vide infra*). Under the optimized PHE conditions of porphyrins, we also tested the η_{H2} of the PSs of porphyrins using the Pt cocatalyst (2 wt%) instead of the CoPyCl cocatalyst (Fig. S3†). The results indicate that the Pt cocatalyst-based PSs showed lower η_{H2} than the PSs of the CoPyCl cocatalyst. Nevertheless, the PSs of porphyrins were tested by varying the concentration of porphyrins (Fig. S4†) and the nature of sacrificial donors such as TEA (Fig. S5†). The output of all the experiments discloses that the PS conditions in Fig. 4 are the best to produce efficient PHE.

To further understand the molecular design of ZnDC(*p*-NI)PP, we evaluated the η_{H_2} of our recently reported efficient ZnD(*p*-NI)PP which contains two NI moieties and lacks the COOH groups. The PS of ZnD(*p*-NI)PP exhibited an η_{H_2} of 3.8 mmol g^{-1} h^{-1} (Fig. S2,† Table 2), which is 10-fold lower than that of the PS of ZnDC(*p*-NI)PP. Similarly, the PHE of methylated ZnDCPP and ZnTCPP porphyrins such as ZnDMCPP and ZnTMCPP, respectively was also tested for better comparison. The η_{H_2} of ZnDMCPP (1.2 mmol g^{-1} h^{-1}) and ZnTMCPP (0.9 mmol g^{-1} h^{-1}) is lower than that of their congener porphyrins, ZnDCPP and ZnTCPP possessing the COOH groups (Fig. S2†). All these results clearly suggest that there would be close contact between COOH of ZnDC(*p*-NI)PP and CoPyCl in the solution of PS. Nevertheless, the Soret band peak of ZnDC(*p*-NI)PP is gradually red-shifted and splits with increasing the concentration of CoPyCl by titration, attributed to the electrostatic interactions between the cationic Co(III) and the negatively charged ZnDC(*p*-NI)PP molecules (Fig. S6†).[38] Thus under light irradiation, the higher performance of ZnDC(*p*-NI)PP in PHE is attributed to the FRET from the NI donor chromophore to the porphyrin acceptor that would promote the long-lived photoexcitation states. At the same time, the anionic form ($-COO^-$) of 4-carboxyphenyl substituents at pH 7.4 enables a faster electron transfer from the porphyrin group to the cationic Co(III) due to electrostatic force.

In order to get more insight into the effect of CoPyCl and AA concentrations on η_{H2}, we have prepared a series of PSs containing ZnDC(*p*-NI)PP and variable concentrations of CoPyCl and AA. From Fig. S7,† it was observed that the concentration of both CoPyCl and AA has also played an important role to optimize the PSs. For achieving high η_{H2}, the PSs must be prepared using 2.0 mM of CoPyCl and 0.4 M of AA. Since PHE of PSs is strongly dependent on pH, the PHE of the ZnDC(*p*-NI)PP PS has been evaluated at different pH values. As seen in Fig. 5, the PS of ZnDC(*p*-NI)PP exhibited the highest η_{H2} of 35.70 mmol g^{-1} h^{-1} at pH 7.4, under likely slightly basic conditions. In contrast, the PS of ZnDC(*p*-NI)PP showed a gradual decrease in η_{H2} when pH

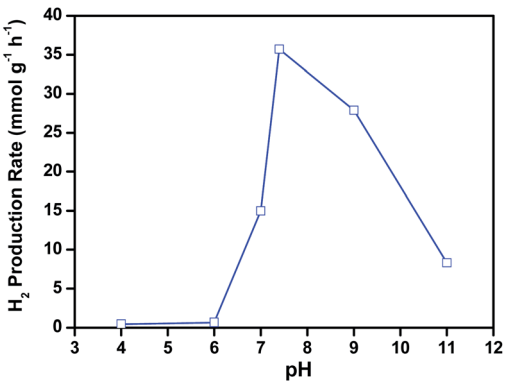

Fig. 5 H_2 production rate of the photocatalytic systems at different pH under irradiation for 5 h: (ZnDC(*p*-NI)PP (10 μM) + CoPyCl (2.0 mM) + AA (0.4 M) + buffer/THF (9 : 1 v/v) at pH 7.4).

either increased or decreased with respect to pH = 7.4. The declined PHE results of the ZnDC(*p*-NI)PP PS under acidic conditions could be attributed to the degradation of AA which hampers the reducing nature of the photoexcited photosensitizer, whereas the rate of formation of the active cobalt hydride catalytic intermediate is low under basic conditions and consequently reduces proton reduction.[40]

Generally, the electron transfer mechanism involved in homogeneous PHE systems comprising a photosensitizer, sacrificial donor and cocatalyst proceeds through either oxidative or reductive quenching pathways. The dominance of the quenching type dictates the multistep electron transfer pathway in PSs. The oxidative quenching mechanism involves the transfer of photoexcited electrons from the photosensitizer to the cocatalyst followed by the reduction of the oxidized photosensitizer back to the original ground state by taking electrons from the sacrificial donor. In the case of the reductive quenching mechanism, the sacrificial donor reduces the excited photosensitizer which further returns to the ground state by transferring electrons to the cocatalyst where proton reduction takes place. Thus, to understand the type of the electron transfer mechanism involved in our PSs, we have performed the quenching studies using CoPyCl and AA as quenchers (Fig. S8–S10†). For instance, the fluorescence emission intensity of ZnDC(*p*-NI)PP is gradually decreased with increasing the concentration of either CoPyCl or AA (Fig. S4†). This indicates that the photoexcited ZnDC(*p*-NI)PP could either efficiently accept electrons from AA or transfer electrons to CoPyCl. The calculated Stern–Volmer quenching constants (K_q) of ZnDC(*p*-NI)PP are 1.9×10^2 M^{-1} s^{-1} and 4.2 M^{-1} s^{-1} for quenchers CoPyCl and AA, respectively (Fig. 6). However, given the high concentration of AA (0.4 M) than the CoPyCl (2.0 mM) used in the PSs, the calculated oxidative and reductive quenching rates of ZnDC(*p*-NI)PP are 38×10^2 s^{-1} and 168×10^2 s^{-1}, respectively. Since the reductive quenching rate is 5 times higher than the oxidative quenching rate, the reductive quenching mechanism can be assigned to the current PSs. Accordingly, the calculated oxidative quenching rates of ZnDCPP and ZnTCPP are 1.6×10^{-2} and 4.6×10^{-2} s^{-1}, respectively whereas the values 0.57×10^{-4} and 0.15×10^{-4} s^{-1} correspond to the quenching rates of ZnDCPP and ZnTCPP, respectively. The reductive quenching rate order of porphyrins is ZnDC(*p*-NI)PP > ZnTCPP > ZnDCPP whereas the order, ZnDC(*p*-NI)PP > ZnDCPP > ZnTCPP represents the oxidative quenching rates of the porphyrins. These quenching rate orders reveal that the ZnDC(*p*-NI)PP porphyrin can efficiently accept electrons from AA, which are further quickly donated to CoPyCl than the control porphyrins ZnDCPP and ZnTCPP. This result is also well consistent with higher PHE results for ZnDC(*p*-NI)PP PS than the PSs of ZnDCPP and ZnTCPP porphyrins.

Based on the optoelectronic, PHE and Stern–Volmer quenching studies, we have proposed a schematic illustration of the electron transfer mechanism involved in the photo-redox cycle for hydrogen production (Fig. 7). Upon light irradiation on NI containing ZnDC(*p*-NI)PP porphyrin (denoted as NI–P–COO^-), the photoexcited NI moiety transfers energy to the porphyrin ring through the IET process, followed by the formation of the photoexcited porphyrin complex [NI–P–COO^-]*. This complex then accepts an electron from AA resulting in reduced [NI–P–COO^-]$^-$ species which further donates two electrons to Co(III)PyCl to give reduced Co(I)PyCl. Finally, the resulting Co(I) species ultimately reduces protons to hydrogen.

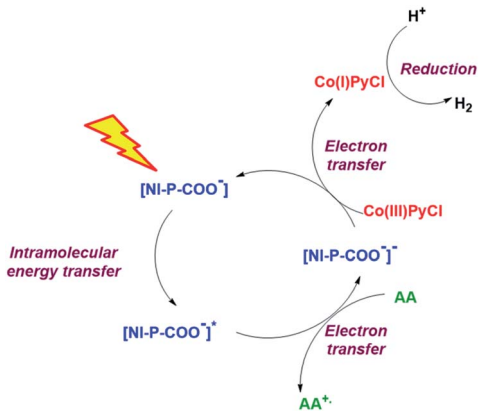

Fig. 7 Schematic illustration of the photo-redox cycle mechanism for PHE with ZnDC(*p*-NI)PP, where NI–P–COO^- represents ZnDC(*p*-NI)PP.

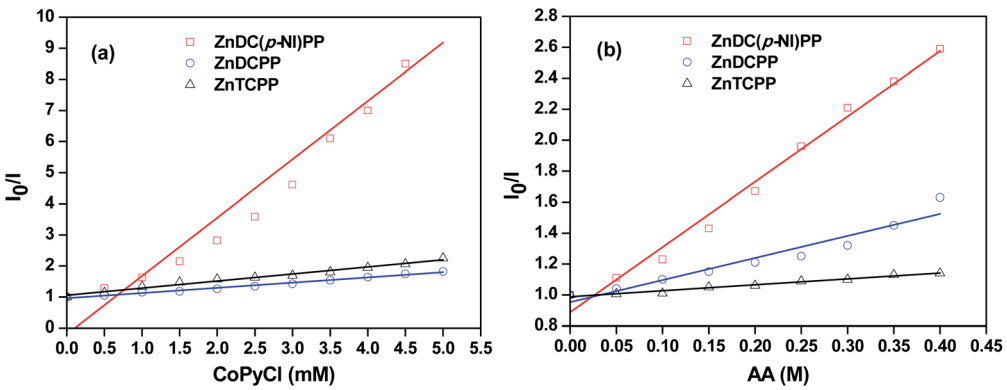

Fig. 6 Stern–Volmer plot of porphyrins (10 μM) with (a) CoPyCl and (b) AA as quenchers in the buffer/THF solution at pH 7.4.

The photoinduced hole–electron pair generation and separation of porphyrins also plays a tremendous role in the transfer of electrons from the excited porphyrins to the cocatalyst and thereby evolves H_2. Thus, additionally, we have performed the photocurrent response studies for the porphyrins. As seen in Fig. S12,† the photocurrent response of the porphyrins is in the following order: ZnDC(*p*-NI)PP > ZnDCPP > ZnTCPP. Among all, ZnDC(*p*-NI)PP porphyrin displayed higher photocurrent response than the congener porphyrins ZnDCPP and ZnTCPP suggesting the efficient photoinduced hole–electron pair separation and migration of electrons from the former porphyrin. This result is also in line with the higher PHE of ZnDC(*p*-NI)PP than the ZnDCPP and ZnTCPP.

Conclusions

In summary, we designed and synthesized a new porphyrin ZnDC(*p*-NI)PP bearing two NI energy donor chromophores and two 4-carboxyphenyl substituents. Absorption and emission spectra revealed that the introduction of two NI moieties at the *meso*-position of the porphyrin moiety enhanced the light harvesting properties, t_F and Φ_F values. Stern–Volmer quenching studies suggested that the electron transfer rate from the porphyrin center to CoPyCl was tremendously enhanced for ZnDC(*p*-NI)PP. This could be ascribed to the stabilized photoexcited states of ZnDC(*p*-NI)PP due to efficient energy transfer from NI moieties to the porphyrin ring. In addition, the anionic form of the 4-carboxyphenyl substituents also facilitated faster electron transfer between the porphyrin centre and the cationic Co(III) due to electrostatic force. Photocurrent response studies also revealed that the ZnDC(*p*-NI)PP showed higher photoinduced charge carrier generation and separation than the ZnDCPP. As a consequence, the homogeneous PS of ZnDC(*p*-NI)PP exhibited improved PHE properties such as η_{H2} of 35.6 mmol g^{-1} h^{-1}, TON of 5958 and AQE of 10.01% than those of ZnDCPP PS (η_{H2} of 4.64 mmol g^{-1} h^{-1} TON of 1397 and AQE of 1.3%) and the typical ZnTCPP porphyrin bearing four COOH (η_{H2} of 2.43 mmol g^{-1} h^{-1} TON of 562 and AQE of 1.0%). Since ZnDC(*p*-NI)PP porphyrin produced very high PHE results, the studies of ZnDC(*p*-NI)PP and graphitic carbon nitride (g-C_3N_4) hybrid materials for H_2 evolution and CO_2 reduction are under investigation in our laboratory.

Conflicts of interest

There are no conflicts to declare.

Acknowledgements

The research was supported by the General Research Fund (HKBU 12304320) from the Hong Kong Research Grants Council, and Initiation Grant for Faculty Niche Research Areas (IG-FNRA) (2020/21)-RC-FNRA-IG/20-21/SCI/06 from Research Committee of Hong Kong Baptist University. W.-Y. W. acknowledges the financial support from the Science, Technology and Innovation Committee of Shenzhen Municipality (JCYJ20180507183413211), the RGC Senior Research Fellowship Scheme (SRFS2021-5S01), the Hong Kong Polytechnic University (1-ZE1C), Research Institute for Smart Energy (RISE) and Ms Clarea Au for the Endowed Professorship in Energy (847S).

Notes and references

1 A. Fujishima and K. Honda, *Nature*, 1972, **238**, 37.
2 Y. Tachibana, L. Vayssieres and J. R. Durrant, *Nat. Photonics*, 2012, **6**, 511.
3 N. Armaroli and V. Balzani, *Angew. Chem., Int. Ed.*, 2007, **46**, 52–66.
4 B. Zhang and L. Sun, *Chem. Soc. Rev.*, 2019, **48**, 2216–2264.
5 M. Kirch, J.-M. Lehn and J.-P. Sauvage, *Helv. Chim. Acta*, 1979, **62**, 1345–1384.
6 I. N. Mills, J. A. Porras and S. Bernhard, *Acc. Chem. Res.*, 2018, **51**, 352–364.
7 X. Zhang, T. Peng and S. Song, *J. Mater. Chem. A*, 2016, **4**, 2365–2402.
8 O. J. Stacey and S. J. A. Pope, *RSC Adv.*, 2013, **3**, 25550–25564.
9 D. Li, J. Shi and C. Li, *Small*, 2018, **14**, 1704179.
10 Y. Shi, A.-F. Yang, C.-S. Cao and B. Zhao, *Coord. Chem. Rev.*, 2019, **390**, 50–75.
11 H. Wang, H. Wang, Z. Wang, L. Tang, G. Zeng, P. Xu, M. Chen, T. Xiong, C. Zhou, X. Li, D. Huang, Y. Zhu, Z. Wang and J. Tang, *Chem. Soc. Rev.*, 2020, **49**, 4135–4165.
12 T.-X. Wang, H.-P. Liang, D. A. Anito, X. Ding and B.-H. Han, *J. Mater. Chem. A*, 2020, **8**, 7003–7034.
13 J. Jayakumar and H.-H. Chou, *ChemCatChem*, 2020, **12**, 689–704.
14 C. Xu, W. Zhang, J. Tang, C. Pan and G. Yu, *Front. Chem.*, 2018, **6**(592).
15 J. Wen, J. Xie, X. Chen and X. Li, *Appl. Surf. Sci.*, 2017, **391**, 72–123.
16 S. W. Cao, J. X. Low, J. G. Yu and M. Jaroniec, *Adv. Mater.*, 2015, **27**, 2150–2176.
17 S. Fukuzumi, Y.-M. Lee and W. Nam, *J. Porphyrins Phthalocyanines*, 2020, **24**, 21–32.
18 K. Ladomenou, M. Natali, E. Iengo, G. Charalampidis, F. Scandola and A. G. Coutsolelos, *Coord. Chem. Rev.*, 2015, **304–305**, 38–54.
19 X. Fang, Q. Shang, Y. Wang, L. Jiao, T. Yao, Y. Li, Q. Zhang, Y. Luo and H.-L. Jiang, *Adv. Mater.*, 2018, **30**, 1705112.
20 Y. Qian, D. Li, Y. Han and H.-L. Jiang, *J. Am. Chem. Soc.*, 2020, **142**, 20763–20771.
21 P. Kumar, R. Boukherroub and K. Shankar, *J. Mater. Chem. A*, 2018, **6**, 12876–12931.
22 J. Yang, H. Yan, X. Zong, F. Wen, M. Liu and C. Li, *Philos. Trans. R. Soc., A*, 2013, **371**, 20110430.
23 C. Lentz, O. Schott, T. Auvray, G. S. Hanan and B. Elias, *Dalton Trans.*, 2019, **48**, 15567–15576.
24 F. Gärtner, S. Denurra, S. Losse, A. Neubauer, A. Boddien, A. Gopinathan, A. Spannenberg, H. Junge, S. Lochbrunner, M. Blug, S. Hoch, J. Busse, S. Gladiali and M. Beller, *Chem.–Eur. J.*, 2012, **18**, 3220–3225.
25 D. Dolui, S. Khandelwal, P. Majumder and A. Dutta, *Chem. Commun.*, 2020, **56**, 8166–8181.

26 J.-W. Wang, W.-J. Liu, D.-C. Zhong and T.-B. Lu, *Coord. Chem. Rev.*, 2019, **378**, 237–261.
27 Z. Han, L. Shen, W. W. Brennessel, P. L. Holland and R. Eisenberg, *J. Am. Chem. Soc.*, 2013, **135**, 14659–14669.
28 P. Zhang, J. Hu, B. Liu, J. Yang and H. Hou, *Chemosphere*, 2019, **219**, 617–635.
29 A. Fihri, V. Artero, M. Razavet, C. Baffert, W. Leibl and M. Fontecave, *Angew. Chem., Int. Ed.*, 2008, **47**, 564–567.
30 P. Zhang, M. Wang, C. Li, X. Li, J. Dong and L. Sun, *Chem. Commun.*, 2010, **46**, 8806–8808.
31 T. Lazarides, M. Delor, I. V. Sazanovich, T. M. McCormick, I. Georgakaki, G. Charalambidis, J. A. Weinstein and A. G. Coutsolelos, *Chem. Commun.*, 2014, **50**, 521–523.
32 G. B. Bodedla, J. Huang, W.-Y. Wong and X. Zhu, *ACS Appl. Nano Mater.*, 2020, **3**, 7040–7046.
33 G. B. Bodedla, L. Li, Y. Che, Y. Jiang, J. Huang, J. Zhao and X. Zhu, *Chem. Commun.*, 2018, **54**, 11614–11617.
34 G. B. Bodedla, G. Tang, J. Zhao and X. Zhu, *Sustainable Energy Fuels*, 2020, **4**, 2675–2679.
35 G. B. Bodedla, D. N. Tritton, X. Chen, J. Zhao, Z. Guo, K. C.-F. Leung, W.-Y. Wong and X. Zhu, *ACS Appl. Energy Mater.*, 2021, **4**, 3945–3951.
36 N. Queyriaux, E. Giannoudis, C. D. Windle, S. Roy, J. Pécaut, A. G. Coutsolelos, V. Artero and M. Chavarot-Kerlidou, *Sustainable Energy Fuels*, 2018, **2**, 553–557.
37 E. Giannoudis, E. Benazzi, J. Karlsson, G. Copley, S. Panagiotakis, G. Landrou, P. Angaridis, V. Nikolaou, C. Matthaiaki, G. Charalambidis, E. A. Gibson and A. G. Coutsolelos, *Inorg. Chem.*, 2020, **59**, 1611–1621.
38 X. Yang, Z. Hu, Q. Yin, C. Shu, X.-F. Jiang, J. Zhang, X. Wang, J.-X. Jiang, F. Huang and Y. Cao, *Adv. Funct. Mater.*, 2019, **29**, 1808156.
39 D. N. Tritton, G. B. Bodedla, G. Tang, J. Zhao, C.-S. Kwan, K. C.-F. Leung, W.-Y. Wong and X. Zhu, *J. Mater. Chem. A*, 2020, **8**, 3005–3010.
40 B. B. Beyene and C.-H. Hung, *Sustainable Energy Fuels*, 2018, **2**, 2036–2043.

